New Gate Driving Technique Using Digital Gate Driver IC to Reduce Both EMI in Specific Frequency Band and Switching Loss in IGBTs

Ryuzo Morikawa, Toru Sai, Katsuhiro Hata, and Makoto Takamiya

The University of Tokyo, Tokyo, Japan

rmori@iis.u-tokyo.ac.jp

***Abstract*— A new gate driving technique using a digital gate driver IC is proposed to reduce both conductive EMI in user-defined specific frequency band and the switching loss in IGBTs to achieve a highly efficient power converter complying with EMI regulations. The reduction is automatically achieved by repeating the switching measurements and exploring optimum gate driving vectors of the digital gate driver using a simulated annealing algorithm. In the double pulse test of IGBT at 20 A and 300 V, the reduction of EMI and the switching loss at four different frequency bands (2 MHz to 5 MHz, 5 MHz to 7.5 MHz, 7.5 MHz to 10 MHz, and 10 MHz to 20 MHz) are demonstrated. At the target frequency band of 7.5 MHz to 10 MHz, compared with the conventional single step gate drive, the proposed digital gate drive reduces the spectrum area by 46 % and the maximum EMI is reduced by −105 dBμV at the same switching loss.**

Keywords— Gate driver, IGBT, Conductive EMI, Optimization

I. INTRODUCTION

In the development process of power converters, the electromagnetic interference (EMI) is a troublesome problem, because the EMI measurement to check pass or fail the EMI regulations is done after the final product of the power converter is completed. When the power converter fails the EMI regulations, two types of measures, hardware-based approach and software-based approach, are considered. In the hardware-based approach, several components including EMI filters and shield plates are added to reduce EMI, which will increase the cost and delay the product development schedule. Therefore, the software-based approach, where the EMI spectrum is tuned using a programmable hardware, is preferred, because it is cheaper and faster than the hardware-based approach.

A programmable gate driver, which controls a gate driving waveform of power transistors during turn-on / off transients with gate driving vectors, is a promising candidate for the programmable hardware for the software-based approach. In the trouble shooting of EMI, EMI reduction in a specific frequency band is often required to satisfy the EMI regulations, for example, reducing EMI in 500 kHz to 1.6 MHz frequency band for AM radio broadcasting in automotive applications [1-2]. The previously reported programmable gate drivers [3-9], however, are not suitable for the EMI reduction in the specific frequency band, because the gate waveform controls are based on the time-domain analysis such as dV_{CE}/dt and d^2V_{CE}/dt^2, where V_{CE} is collector-to-emitter voltage of IGBT. In [1-2], the switching loss (E_{LOSS}) is not evaluated, though the EMI reduction in the specific frequency band is achieved. Both EMI and E_{LOSS} should be considered, because they are in a trade-off relationship [3].

To solve the problems, in this paper, a new gate driving technique using a digital gate driver (DGD) IC [10] based on frequency-domain analysis of V_{CE} is proposed for the first time to reduce both conductive EMI in user-defined specific frequency band and E_{LOSS} in IGBTs, thereby achieving a highly efficient power converter complying with EMI regulations. The optimization of the gate driving waveforms to solve the trade-off between EMI and E_{LOSS} is automatically done using a software. In the measurements, the reduction of EMI and E_{LOSS} at four different frequency bands (2 MHz to 5 MHz, 5 MHz to 7.5 MHz, 7.5 MHz to 10 MHz, and 10 MHz to 20 MHz) are demonstrated.

II. PROPOSED GATE DRIVING TECHNIQUE USING DIGITAL GATE DRIVER IC

In general, the conductive EMI is evaluated by measuring the frequency spectrum of the input voltage of the continuously operating power converter. In this paper, however, to simplify the measurement setup, V_{CE} waveform during turn-off measured in the double pulse test is used to obtain V_{CE} spectrum. The details will be explained later.

The measurement setup and the gate waveform optimization method for DGD are the same as [11] except for the length of the gate driving vector for DGD, time step of DGD, and the object function for the optimization. Fig. 1 shows a circuit schematic of the measurement setup for the double pulse test of IGBT (2MBI100TA-060-50, 600 V, 100 A) at 300 V. In order to realize a programmable 63-level drivability in DGD, 63 parallel transistors are connected to the gate of IGBT and a 6-bit control signal is applied to specify the number of activated PMOS (NMOS) transistors, n_{PMOS} (n_{NMOS}) [10]. Fig. 2 (a) shows the gate driving vectors and waveforms in the 6-bit DGD. In this paper, the gate driving vectors are

defined as (n_1, n_2, n_3, … , n_8) , where n_1, n_2, and n_8 are integers from 0 to 63. Eight 200-ns time steps for turn-off are used, because four 400-ns time steps in [11] were not enough. Fig. 2 (b) shows the gate driving vectors and waveforms of the conventional single-step gate drive for comparison.

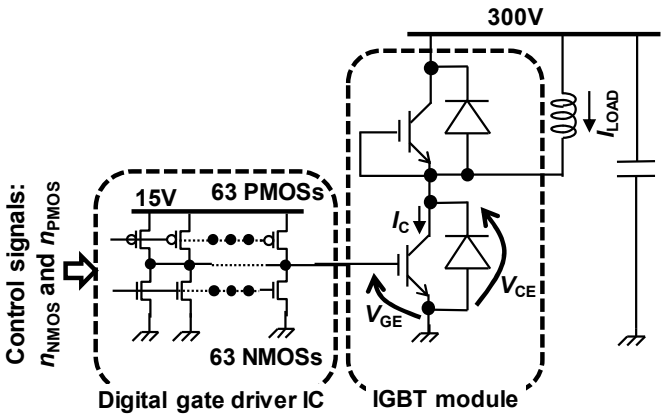

Fig. 1. Circuit schematic for double pulse test of IGBT.

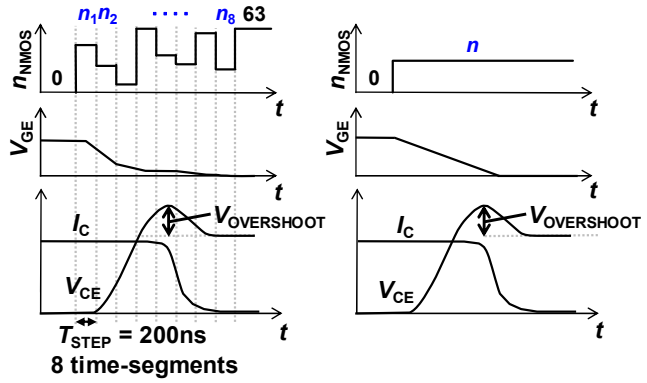

(a) (b)

Fig. 2. Gate driving vectors and waveforms. (a) Proposed 6-bit digital gate driver. (b) Conventional single-step gate drive for comparison.

Fig. 3 shows a method to obtain V_{CE} spectrum from V_{CE} waveform measured in the double pulse test. First, a V_{CE} rise edge waveform of 2-µs duration during turn-off is extracted from the double pulse test, and it is flipped horizontally to make the rise edge waveform. Then, the fall and rise edge waveforms are merged and repeated m times (e.g. m = 20) to make a repetitive waveform. Finally, a spectrum is obtained by FFT of the repetitive waveform. In order to evaluate EMI in the user-defined frequency band from f_{START} to f_{END}, a spectrum area ($A_{SPECTRUM}$) is defined as shown in Fig. 3 and Eqs. (1) to (4). $A_{SPECTRUM}$ is the area shown yellow in Fig. 3 and reducing $A_{SPECTRUM}$ means that EMI in the target band is reduced.

$$A_{SPECTRUM} = \int_{F_{START}}^{F_{END}} VA_{CE}\,dF \tag{1}$$

$$F = \log_{10}\left(\frac{f}{1[MHz]}\right) \tag{2}$$

$$F_{START} = \log_{10}\left(\frac{f_{START}}{1[MHz]}\right) \tag{3}$$

$$F_{END} = \log_{10}\left(\frac{f_{END}}{1[MHz]}\right) \tag{4}$$

where VA_{CE} is the spectrum amplitude of V_{CE} in units of dBµV and f is the frequency. Object function (f_{OBJ}) to be minimized in the optimization using the simulated annealing algorithm [10-11] is defined as

$$f_{OBJ} = \sqrt{\left(\frac{A_{SPECTRUM}}{A_{SPECTRUM,MAX}}\right)^2 + \left(\frac{E_{LOSS}}{E_{LOSS,MAX}}\right)^2} \tag{5}$$

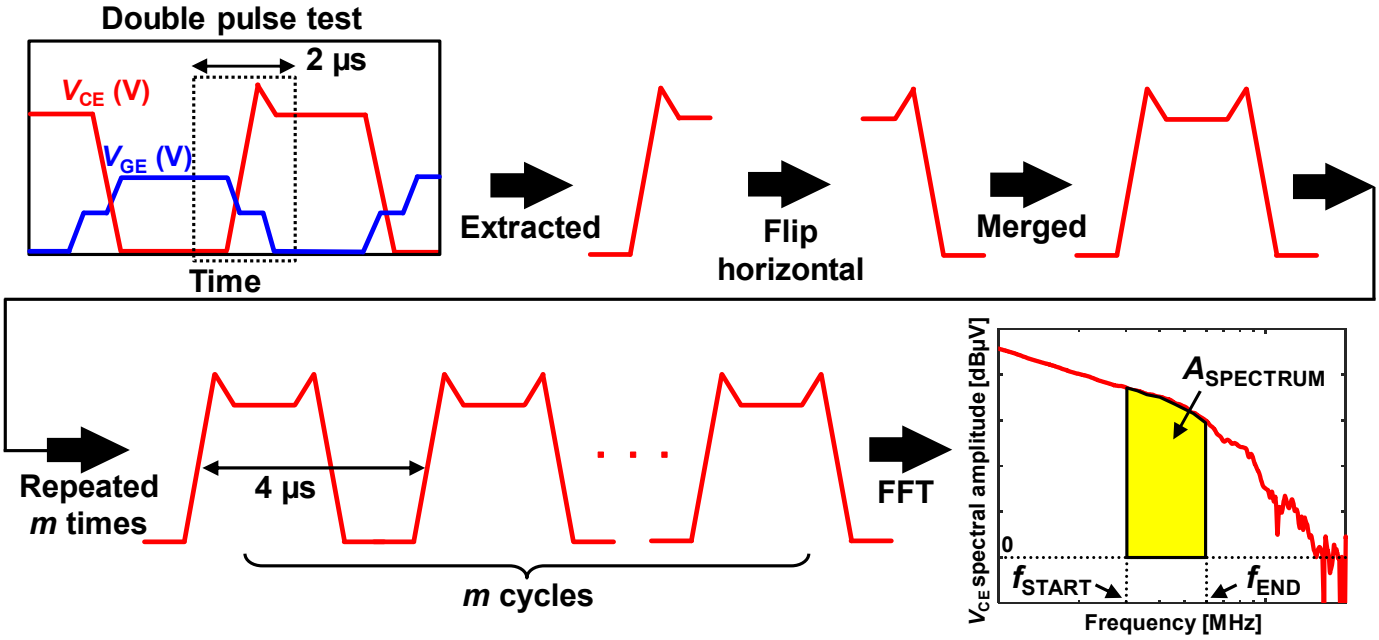

Fig. 3. Method to obtain V_{CE} spectrum from V_{CE} waveform measured in double pulse test.

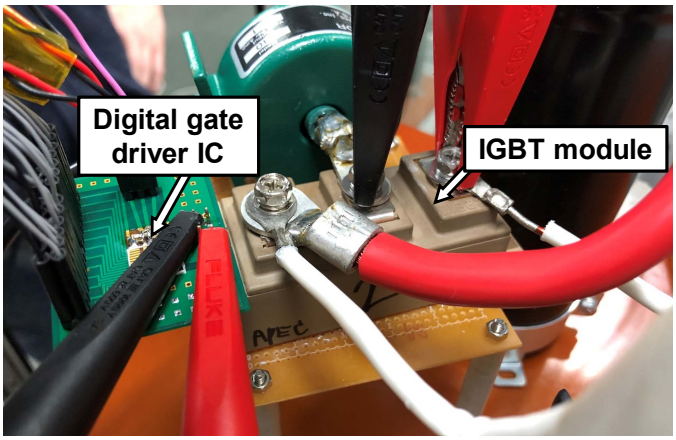

Fig. 4. Photo of measurement setup.

where the subscript MAX signifies the maximum of the corresponding quantity. Compared with [11], only the definition of f_{OBJ} is changed and the optimization algorithm is the same. The gate driving vectors (n_1, n_2, n_3, … , n_8) are globally and automatically optimized by repeating the double pulse test approximately 5000 times using LabVIEW and MATLAB, which takes approximately 40 minutes.

Fig. 4 shows the photo of the measurement setup. The load current is 20 A. The double pulse test measurements were made at room temperature.

III. Measured Results

To demonstrate the benefits of flexibility of the proposed software-based EMI solution, the optimization of the gate driving waveforms to solve the trade-off between EMI and E_{LOSS} at four different frequency bands (2 MHz to 5 MHz, 5 MHz to 7.5 MHz, 7.5 MHz to 10 MHz, and 10 MHz to 20 MHz) are shown. Table I summarizes the measured results at the four different frequency bands. Figs. 5, 8, 11, and 14 show the measured E_{LOSS} vs. $A_{SPECTRUM}$ of the conventional single-step gate drive in Fig. 2 (b) with varied n from 5 (minimum in this paper) to 63 (maximum) and the proposed gate drive in Fig. 2 (a) optimized for the target frequency bands of 2 MHz to 5 MHz, 5 MHz to 7.5 MHz, 7.5 MHz to 10 MHz, and 10 MHz to 20 MHz, respectively. The dotted concentric curves show the contour of f_{OBJ} defined in Eq. (5). Figs. 6, 9, 12, and 15 show the measured comparison of V_{CE}

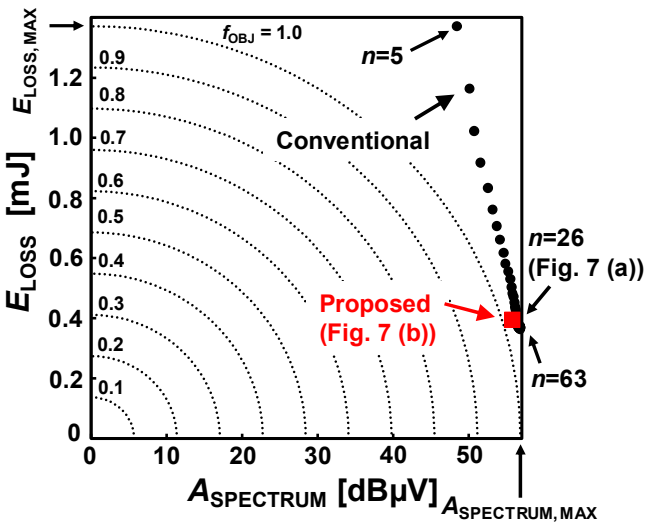

Fig. 5. Measured E_{LOSS} vs. $A_{SPECTRUM}$ of conventional single-step gate drive and proposed gate drive optimized for target frequency bands of 2 MHz to 5 MHz.

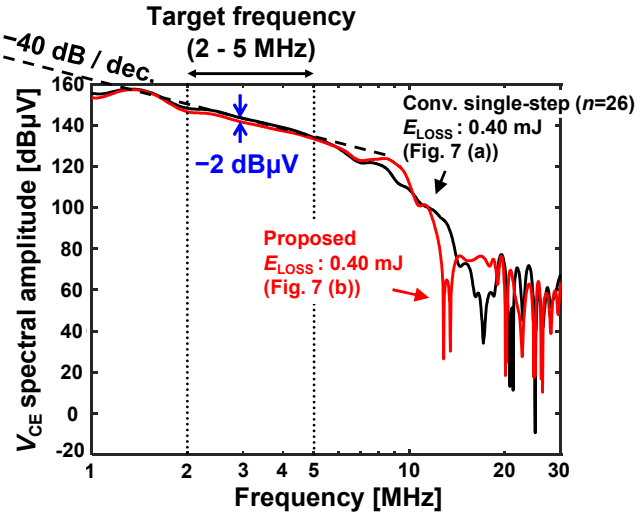

Fig. 6. Measured comparison of V_{CE} spectrums of conventional single-step gate drive and proposed gate drive optimized for target frequency bands of 2 MHz to 5 MHz under same E_{LOSS} condition.

TABLE I. Summary of Measured Results at Four Different Frequency Bands.

Target frequency	E_{LOSS} vs. $A_{SPECTRUM}$	V_{CE} spectrum	Waveforms	Reduction of $A_{SPECTRUM}$ at same E_{LOSS}	Max EMI reduction	Benefits of proposal
2 - 5 MHz	Fig. 5	Fig. 6	Fig. 7	−1.2 %	−2 dBμV	Small
5 - 7.5 MHz	Fig. 8	Fig. 9	Fig. 10	−21 %	−57 dBμV	Large
7.5 - 10 MHz	Fig. 11	Fig. 12	Fig. 13	−46 %	−105 dBμV	Largest
10 - 20 MHz	Fig. 14	Fig. 15	Fig. 16	−8.4 %	−61 dBμV	Medium

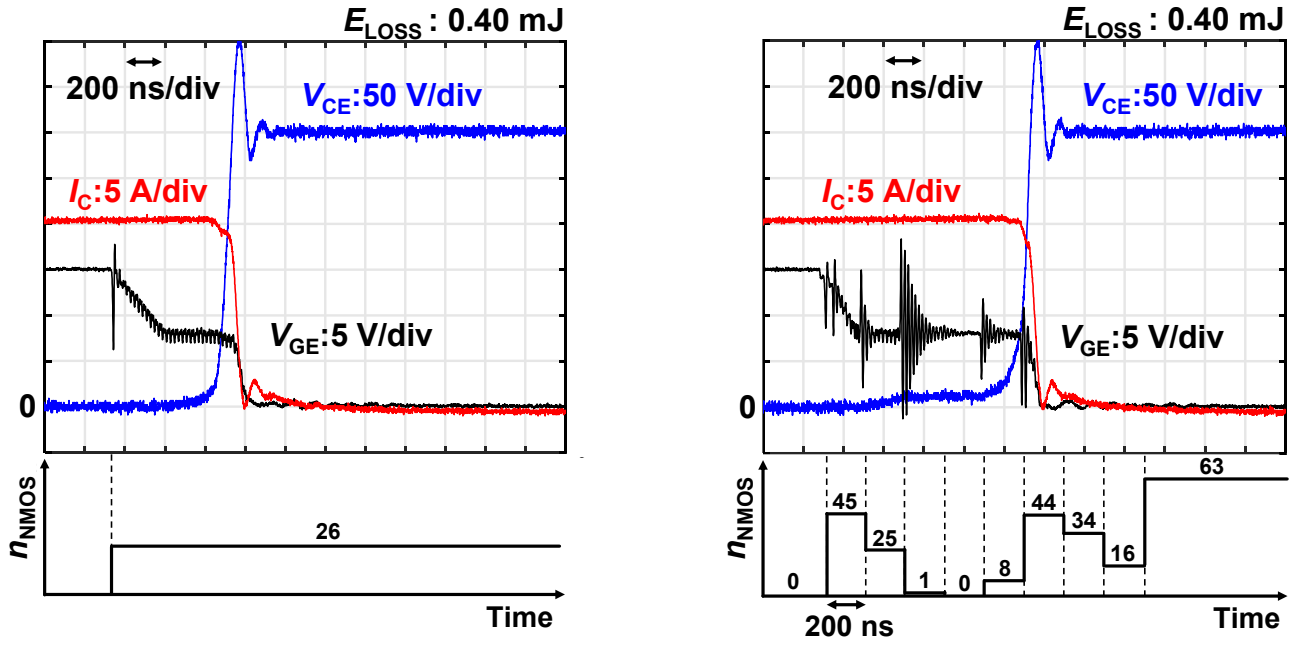

Fig. 7. Gate driving vectors and measured waveforms under same E_{LOSS} condition. (a) Conventional single-step gate drive. (b) Proposed gate drive optimized for target frequency bands of 2 MHz to 5 MHz.

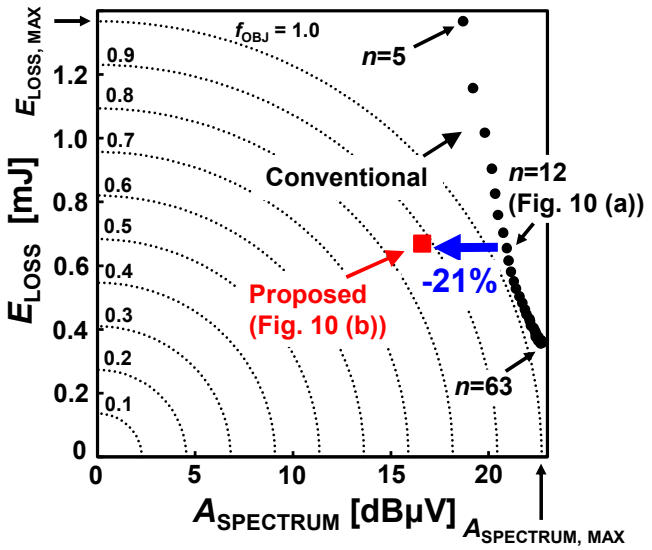

Fig. 8. Measured E_{LOSS} vs. $A_{SPECTRUM}$ of conventional single-step gate drive and proposed gate drive optimized for target frequency bands of 5 MHz to 7.5 MHz.

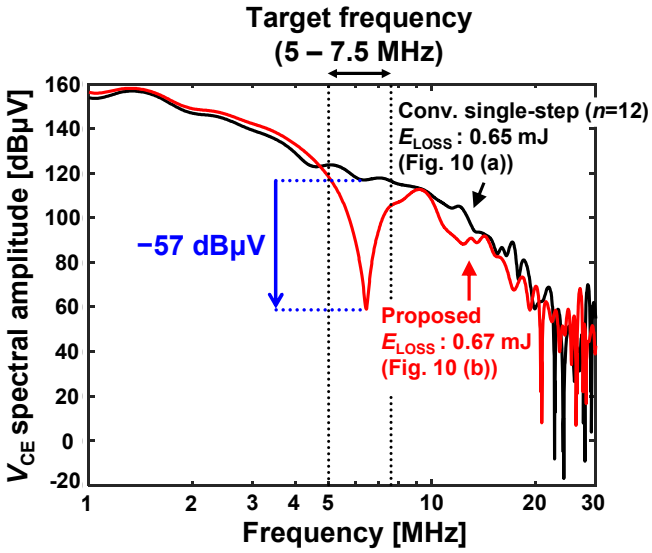

Fig. 9. Measured comparison of V_{CE} spectrums of conventional single-step gate drive and proposed gate drive optimized for target frequency bands of 5 MHz to 7.5 MHz under same E_{LOSS} condition.

spectrums of the conventional single-step gate drive and the proposed gate drive under the same E_{LOSS} condition optimized for the target frequency bands of 2 MHz to 5 MHz, 5 MHz to 7.5 MHz, 7.5 MHz to 10 MHz, and 10 MHz to 20 MHz, respectively. Figs. 7, 10, 13, and 16 show the gate driving vectors and measured waveforms of gate-to-emitter voltage (V_{GE}), collector current (I_C), and V_{CE} in the conventional single-step gate drive and the proposed gate drive under the same E_{LOSS} condition optimized for the target frequency bands of 2 MHz to 5 MHz, 5 MHz to 7.5 MHz, 7.5 MHz to 10 MHz, and 10 MHz to 20 MHz, respectively.

Of the four target frequency bands, 5 MHz to 7.5 MHz frequency band is explained, which is the easiest to understand. In Fig. 8, in the conventional single-step gate drive, when n is increased from 5 to 63, E_{LOSS} is reduced, while $A_{SPECTRUM}$ is increased, because the rise time of V_{CE} is reduced. At the same E_{LOSS}, $A_{SPECTRUM}$ of the proposed gate

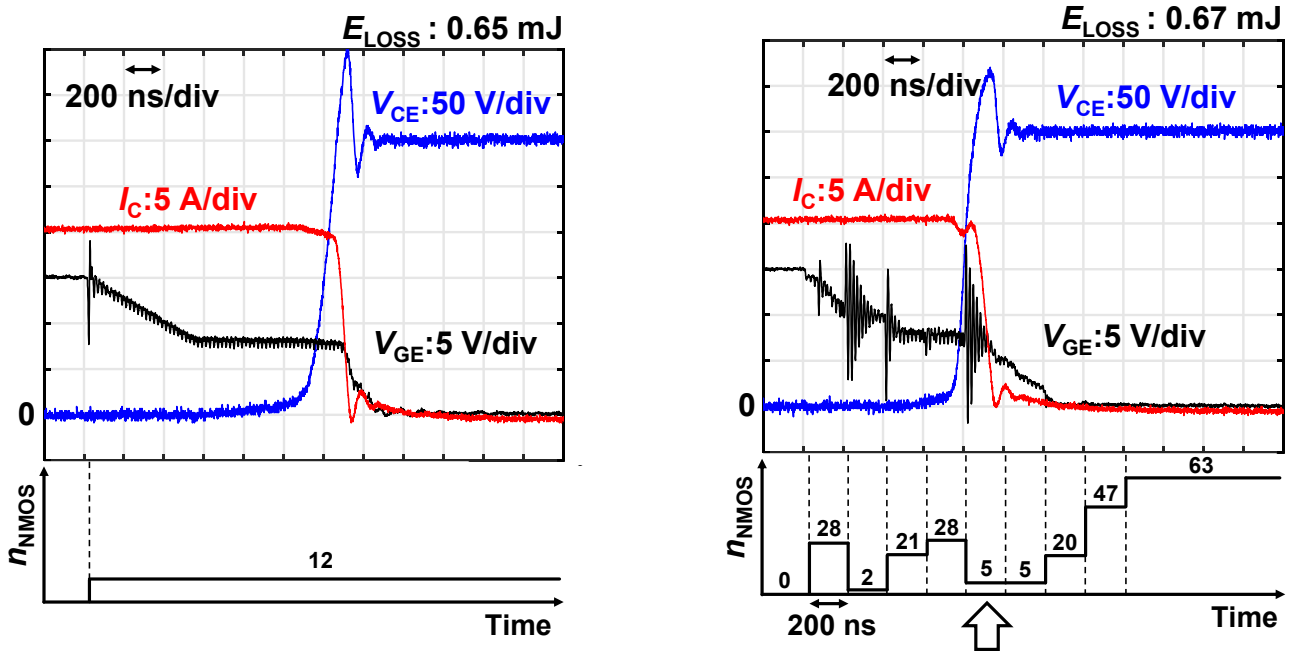

(a) (b)

Fig. 10. Gate driving vectors and measured waveforms under same E_{LOSS} condition. (a) Conventional single-step gate drive. (b) Proposed gate drive optimized for target frequency bands of 5 MHz to 7.5 MHz.

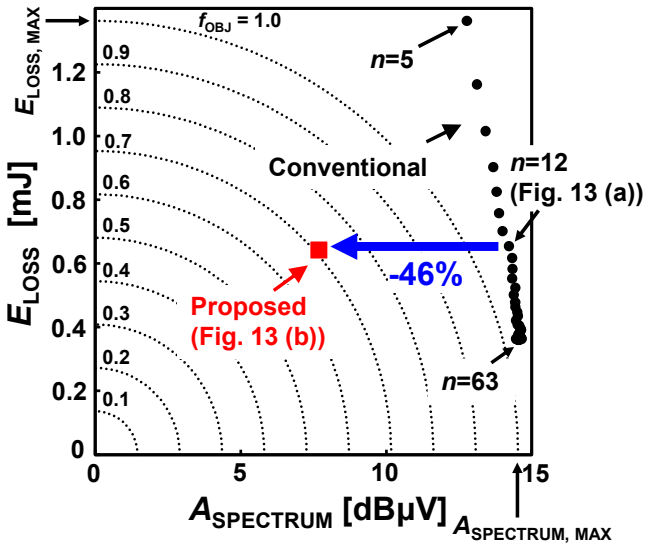

Fig. 11. Measured E_{LOSS} vs. $A_{SPECTRUM}$ of conventional single-step gate drive and proposed gate drive optimized for target frequency bands of 7.5 MHz to 10 MHz.

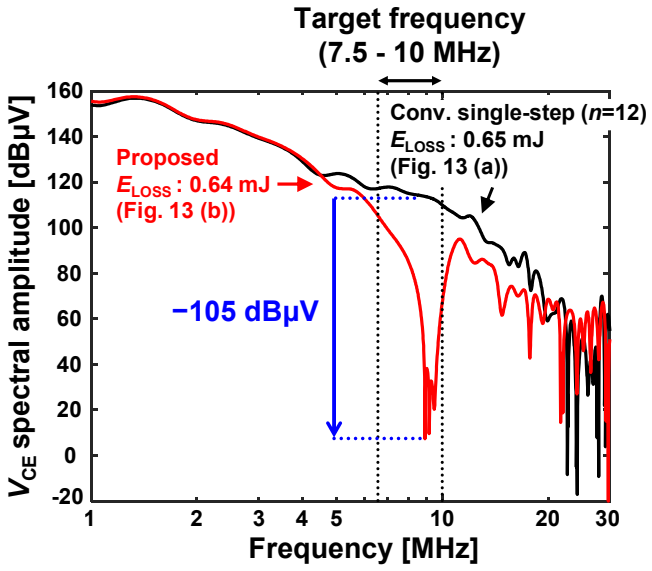

Fig. 12. Measured comparison of V_{CE} spectrums of conventional single-step gate drive and proposed gate drive optimized for target frequency bands of 7.5 MHz to 10 MHz under same E_{LOSS} condition.

drive is reduced by 21 % compared with the conventional single-step gate drive with n = 12. In Figs. 9 and 10, the conventional single-step gate drive (n = 12) and the proposed gate drive under the same E_{LOSS} condition are compared in detail. In Fig. 9, compared with the conventional single-step gate drive, the proposed gate drive clearly reduces EMI at the target frequency band of 5 MHz to 7.5 MHz and the maximum reduction of VA_{CE} is −57 dBμV. In the proposed gate drive, please note that EMI is certainly reduced at the target frequency band of 5 MHz to 7.5 MHz, while EMI may increase outside the range of the target frequency band. Figs. 10 (a) and (b) show the gate driving vectors and measured waveforms in the conventional single-step gate drive and the proposed gate drive, respectively. The gate driving vectors in

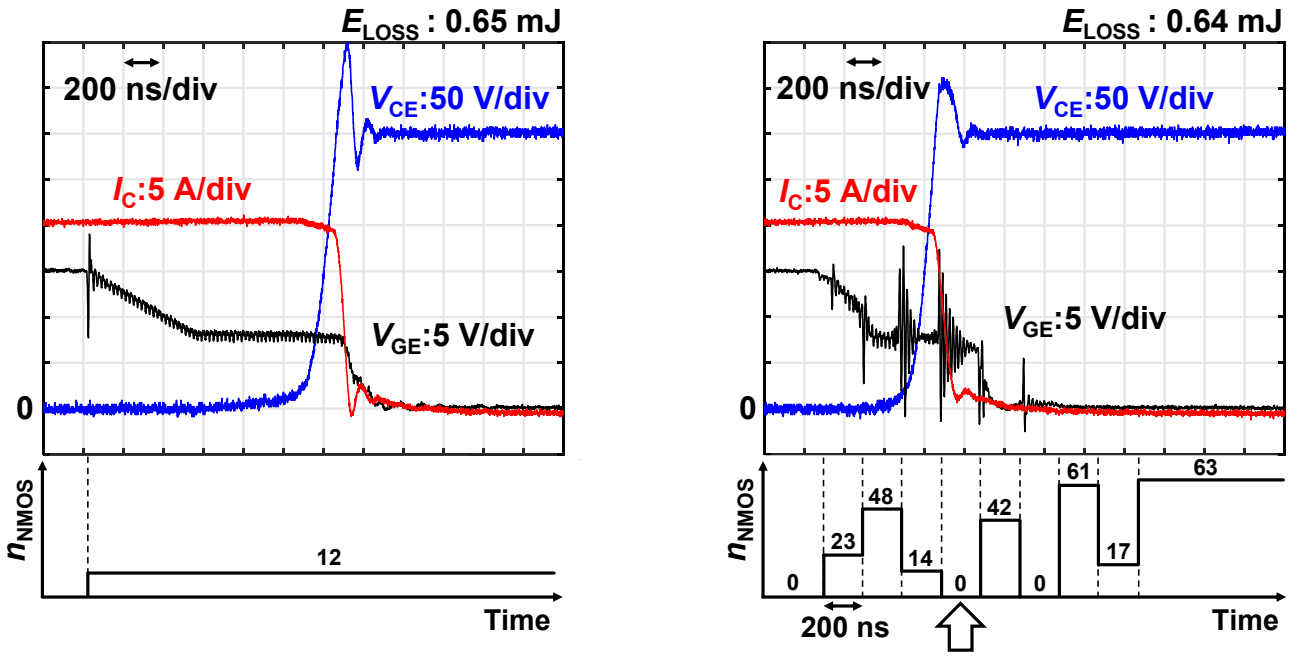

(a) (b)

Fig. 13. Gate driving vectors and measured waveforms under same E_{LOSS} condition. (a) Conventional single-step gate drive. (b) Proposed gate drive optimized for target frequency bands of 7.5 MHz to 10 MHz.

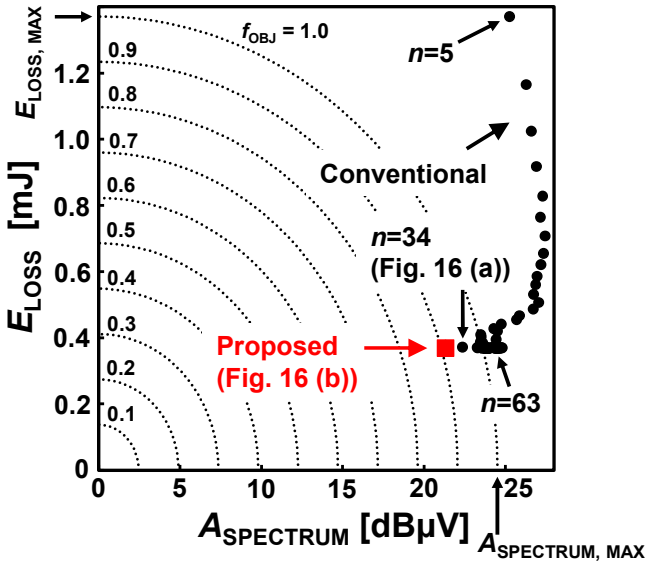

Fig. 14. Measured E_{LOSS} vs. $A_{SPECTRUM}$ of conventional single-step gate drive and proposed gate drive optimized for target frequency bands of 10 MHz to 20 MHz.

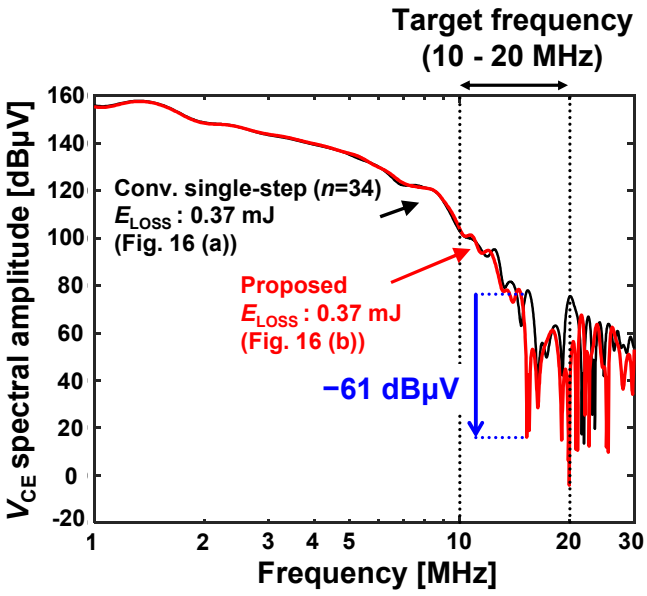

Fig. 15. Measured comparison of V_{CE} spectrums of conventional single-step gate drive and proposed gate drive optimized for target frequency bands of 10 MHz to 20 MHz under same E_{LOSS} condition.

Fig. 10 (b) are automatically obtained using the optimization algorithm. In the proposed gate drive, the reason for the reduction of VA_{CE} at the target frequency band of 5 MHz to 7.5 MHz in Fig. 9 is estimated to be $n_5 = 5$ (the arrow in Fig. 10 (b)), because dV_{CE}/dt during the overshoot of V_{CE} is reduced by the transient small gate driving current ($n_5 = 5$).

Table I summarizes the reduction of $A_{SPECTRUM}$ at the same E_{LOSS} and the maximum EMI (VA_{CE}) reduction of the proposed gate drive compared with the conventional single-step gate at the four target frequency bands. At the target frequency band of 7.5 MHz to 10 MHz, the benefit of the proposed gate drive is the largest. $A_{SPECTRUM}$ is reduced by 46 % and the maximum reduction of VA_{CE} is −105 dBμV. At

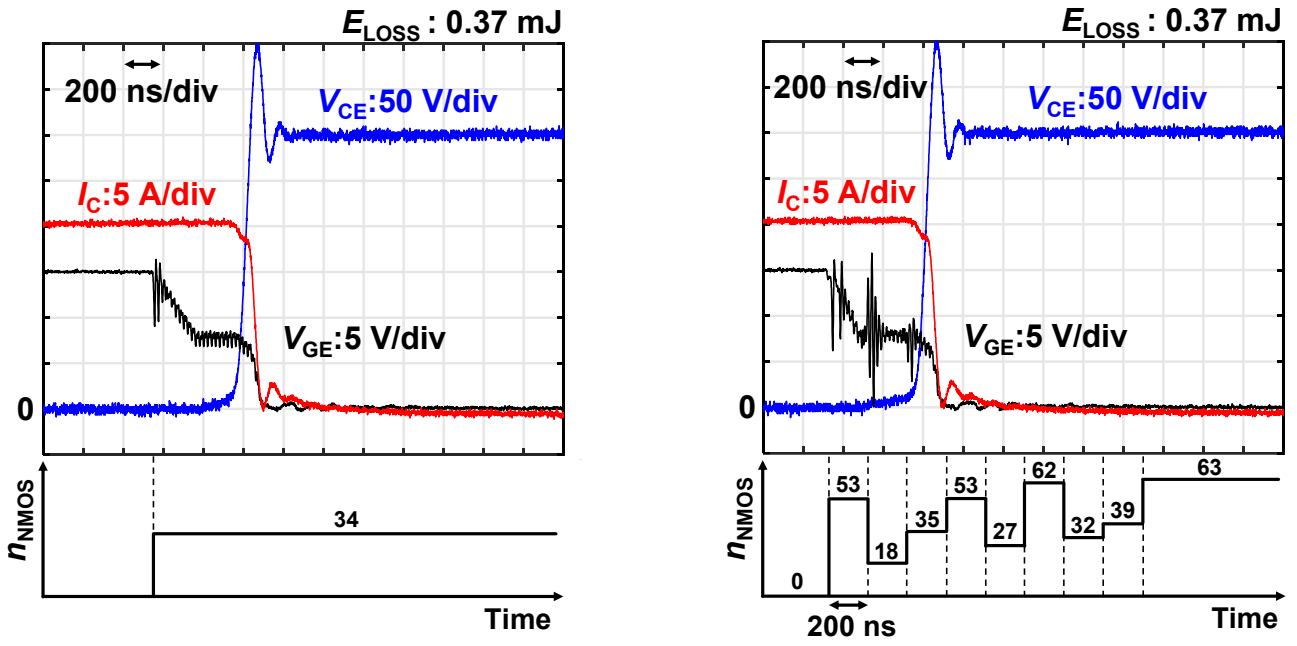

Fig. 16. Gate driving vectors and measured waveforms under same E_{LOSS} condition. (a) Conventional single-step gate drive. (b) Proposed gate drive optimized for target frequency bands of 10 MHz to 20 MHz.

the target frequency band of 5 MHz to 7.5 MHz, the benefit of the proposed gate drive is the second largest.

In contrast, at the target frequency band of 2 MHz to 5 MHz, the benefit of the proposed gate drive is the smallest. $A_{SPECTRUM}$ is reduced by 1.2 % and the maximum reduction of VA_{CE} is −2 dBμV. The reason why the proposed gate drive is not effective at the target frequency band of 2 MHz to 5 MHz is discussed. As shown in Fig. 6, the gradient of V_{CE} spectrums at the target frequency band of 2 MHz to 5 MHz is −40 dB / dec., which derives from the repetitive trapezoidal waveforms [1][4]. To reduce EMI at the target frequency band of 2 MHz to 5 MHz, the rise time and the fall time of V_{CE} waveform should be increased. The increase of the rise / fall time of V_{CE} waveform, however, is not accepted in the optimization as shown in Eq. (5), because it increases E_{LOSS}. Therefore, the benefit of the proposed gate drive is the smallest at the target frequency band of 2 MHz to 5 MHz. The benefit of the proposed gate drive is also small at the target frequency band of 10 MHz to 20 MHz, because the time step of the proposed gate drive is 200 ns corresponding to 5 MHz and the target frequency band is beyond 10 MHz.

In conclusion, the proposed gate drive is effective at the target frequency band between 5 MHz to 10 MHz, because the time step of the proposed gate drive is 200 ns. In order to reduce the high frequency EMI beyond 10 MHz, the time step should be reduced.

IV. Conclusions

To reduce both conductive EMI in the specific frequency band and E_{LOSS}, the new gate driving technique using DGD based on the frequency-domain analysis of V_{CE} is proposed. At the target frequency band of 7.5 MHz to 10 MHz, compared with the conventional single step gate drive, the proposed digital gate drive reduces $A_{SPECTRUM}$ by 46 % and the maximum EMI is reduced by −105 dBμV at the same E_{LOSS}. The proposed gate drive is effective at the target frequency band between 5 MHz to 10 MHz, because the time step of the proposed gate drive is 200 ns. In order to reduce the high frequency EMI beyond 10 MHz, the time step should be reduced.

References

[1] S. Ogasawara, T. Igarashi, H. Funato, and M. Hara, "Optimization of switching transient waveform to reduce EMI noise in a selective frequency band," in *Proc. IEEE Energy Conversion Congress and Exposition*, Sep. 2009, pp. 1679–1684.

[2] T. Mori, H. Funato, S. Ogasawara, F. Okazaki, and Y. Hirota, "H-bridge step-down converter applied proposed switching transient waveform modification to reduce specific harmonics," in *Proc. IEEE International Conference on Renewable Energy Research and Applications*, Nov. 2012, pp. 1–6.

[3] J. Kagerbauer and T. Jahns, "Development of an active dv/dt control algorithm for reducing inverter conducted EMI with minimal impact on switching losses," in *Proc. IEEE Power Electronics Specialists Conference*, Oct. 2007, pp. 894–900.

[4] N. Oswald, B. Stark, D. Holliday, C. Hargis, and B. Drury, "Analysis of shaped pulse transitions in power electronic switching waveforms for reduced EMI generation," *IEEE Trans. on Industry Applications*, vol. 47, issue 5, pp. 2154–2165, July 2011.

[5] N. Oswald, P. Anthony, N. McNeill, and B. Stark, "An experimental investigation of the tradeoff between switching losses and EMI generation with hard-switched all-Si, Si-SiC, and all-SiC device combinations," *IEEE Trans. on Power Electronics*, vol. 29, no. 5, pp. 2393–2407, Aug. 2013.

[6] M. Blank, T. Gluck, A. Kugi, and H. Kreuter, "Digital slew rate and S-shape control for smart power switches to reduce EMI generation,"

IEEE Trans. on Power Electronics, vol. 30, no. 9, pp. 5170–5180, Oct. 2014.

[7] X. Yang, Y. Yuan, X. Zhang, and P. Palmer, "Shaping high-power IGBT switching transitions by active voltage control for reduced EMI generation," *IEEE Trans. on Industry Applications*, vol. 51, issue 2, pp. 1669–1677, March-April 2015.

[8] S. Walder, X. Yuan, I. Laird, J. Dalton, "Identification of the temporal source of frequency domain characteristics of SiC MOSFET based power converter waveforms," in *Proc. IEEE Energy Conversion Congress and Exposition*, Sep. 2016, pp. 1–8.

[9] H. Dymond, J. Wang, D. Liu, J. Dalton, N. McNeill, D. Pamunuwa, S. Hollis, and B. Stark, "A 6.7-GHz active gate driver for GaN FETs to combat overshoot, ringing, and EMI," *IEEE Trans. on Power Electronics*, vol. 33, no. 1, pp. 581–594, Mar. 2017.

[10] K. Miyazaki, S. Abe, M. Tsukuda, I. Omura, K. Wada, M. Takamiya, and T. Sakurai, "General-purpose clocked gate driver IC with programmable 63-level drivability to optimize overshoot and energy loss in switching by a simulated annealing algorithm," *IEEE Trans. on Industry Applications*, vol. 53, issue 3, pp. 2350–2357, May-Jun. 2017.

[11] T. Sai, K. Miyazaki, H. Obara, T. Mannen, K. Wada, I. Omura, M. Takamiya, and T. Sakurai, "Load current and temperature dependent optimization of active gate driving vectors," in *Proc. IEEE Energy Conversion Congress and Exposition*, Sep. 2019, pp. 3292–3297.